

# Ozone Reactions with Olefins and Alkynes: Kinetics, Activation Energies, and Mechanisms

Yan Wang, Eva M. Rodríguez, Daniel Rentsch, Zhimin Qiang, and Urs von Gunten\*



Cite This: *Environ. Sci. Technol.* 2025, 59, 4733–4744



Read Online

ACCESS |



Metrics & More



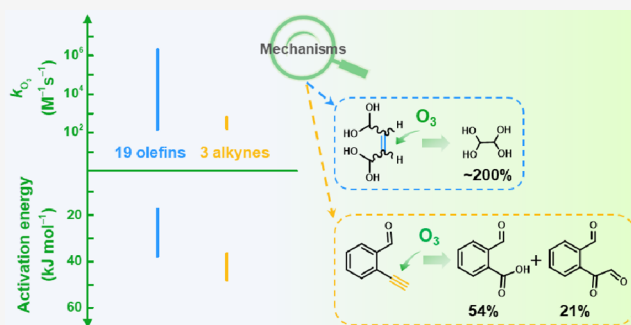
Article Recommendations



Supporting Information

**ABSTRACT:** The temperature dependence of the kinetics and the mechanisms of ozone reactions with 19 olefins and 3 alkynes were investigated. The second-order rate constants ( $k_{O_3}$ ) for ozone reactions with olefins were mostly in the range of  $10^3$ – $10^6$   $M^{-1} s^{-1}$ , with activation energies of 17.4–37.7  $kJ mol^{-1}$ . In comparison, alkynes had lower  $k_{O_3}$  ( $\sim 10^2$   $M^{-1} s^{-1}$ ) and higher activation energies (36.7–48.1  $kJ mol^{-1}$ ). Reactivities of both olefins and alkynes are mainly influenced by inductive effects of substituents, with steric effects observed for cyclic olefins. 2-Buten-1,4-dial (BDA), synthesized with a novel method, is a toxic olefinic oxidation product from phenols. Its *cis*- and *trans*-isomers show distinct reactivities with ozone, with  $k_{O_3}$  (20 °C) of  $3.0 \times 10^3$  and  $1.2 \times 10^4$   $M^{-1} s^{-1}$ , respectively. Two mols of glyoxal were formed per mol of ozonated BDA, with a slow release of the second mol from an  $\alpha$ -hydroxyalkylhydroperoxide intermediate. 2-Ethynylbenzaldehyde reacts with ozone with a stoichiometry of 1:1 and  $k_{O_3}$  (20 °C) =  $1.6 \times 10^2$   $M^{-1} s^{-1}$ . Ozone attacks the ethynyl group, yielding a carboxyl product (2-carboxybenzaldehyde, 54%), an aldehyde product (phthalaldehyde), and a dicarbonyl product with a stoichiometric release of  $H_2O_2$  (21%). This study provides kinetic and mechanistic information for assessing the abatement of olefin- and alkyne-containing micropollutants by ozonation at various temperatures.

**KEYWORDS:** ozonation, olefins, alkynes, reaction kinetics, activation energy, transformation mechanism, substituent effect



## 1. INTRODUCTION

Ozone and other chemical oxidants have been widely applied for inactivation of microorganisms and oxidation of pollutants in water treatment.<sup>1–3</sup> Ozone effectively oxidizes a large variety of organic compounds, and there is a significant body of kinetic and mechanistic information for these reactions.<sup>4</sup> Ozone reactions with organic compounds typically follow second-order kinetics, first-order in both ozone and the organic compounds.<sup>5</sup> Despite its effectiveness, ozonation cannot achieve complete mineralization of organic compounds, which results in the formation of transformation products.<sup>4</sup> Nevertheless, transformation products of bioactive compounds have typically much lower biological activities than their parent compounds.<sup>3,6</sup>

Ozone is an electrophile and preferably attacks electron-rich functional groups (e.g., olefins, activated aromatic compounds, neutral amines, and reduced sulfur compounds).<sup>1</sup> Natural organic matter contains some olefinic moieties<sup>7</sup> and algal blooms release olefin-containing compounds (e.g., microcystins<sup>8</sup> and some taste and odor compounds<sup>9</sup>). Many synthetic organic compounds such as pharmaceuticals,<sup>2</sup> pesticides,<sup>10,11</sup> and industrial chemicals<sup>12,13</sup> also contain olefinic moieties. Reactivities of ozone with olefins vary significantly based on substituents, with second-order rate constants ( $k_{O_3}$ ) varying by

up to 8 orders of magnitude ( $10^{-1}$  to  $10^7$   $M^{-1} s^{-1}$ ).<sup>4</sup> However, information on the ozone reactivity of olefins with electron-withdrawing substituents remains limited, particularly for  $\alpha,\beta$ -unsaturated carbonyl compounds raising toxicological concerns.<sup>14,15</sup> Alkynes, another class of unsaturated compounds, also react with ozone.<sup>16,17</sup> The ethynyl moiety is an important functional group in some micropollutants (e.g., propylamide and 17 $\alpha$ -ethynylestradiol).<sup>16</sup> The ozonolysis of alkynes in the gas phase and organic solvents has been extensively studied.<sup>17–19</sup> However, there is limited information about the kinetics and mechanisms of ozone reactions with alkynes in aqueous solutions.

In real treatment systems, temperatures in the range of 1–30 °C can be observed, causing  $k_{O_3}$  to deviate significantly from standard laboratory conditions at  $\sim 20$  °C and thus needing

Received: July 11, 2024

Revised: January 5, 2025

Accepted: February 14, 2025

Published: February 28, 2025



estimations.<sup>20</sup> So far, information about the temperature dependence (activation energy) of ozone reactions is scarce. Activation energies for ozone consumption in different water types ranged from 65 to 70 kJ mol<sup>-1</sup>,<sup>21</sup> while for inactivation of microorganisms like *Escherichia coli*, *Bacillus subtilis* (*B. subtilis*) spores, and the bacteriophage MS2 were 37.1,<sup>22</sup> 42.1,<sup>23</sup> and 12.2–23.4 kJ mol<sup>-1</sup> (pH-dependent),<sup>24</sup> respectively. For ozone reactions with organic compounds with  $k_{O_3} \leq 10^3$  M<sup>-1</sup> s<sup>-1</sup>, activation energies mostly ranged from 35 to 50 kJ mol<sup>-1</sup>.<sup>25–27</sup> In a recent study on abatement of 51 micropollutants in a pilot-scale ozonation of lake water at 6 °C,  $k_{O_3}$  were calculated based on activation energies for compounds with similar structures, providing a rough estimate.<sup>20</sup> However, many studies did not consider the temperature for micropollutant abatement during ozonation under realistic conditions. Overall, there is a significant lack of data on the activation energies, especially for ozone reactions with olefins, alkynes, and nitrogen-containing compounds. Activation energies can be calculated using the Arrhenius equation with  $k_{O_3}$  determined at various temperatures from the slope of a plot of the  $\ln k_{O_3}$  as a function of the temperature (eqs 1 and 2).<sup>28</sup>

$$k_{O_3} = A \exp\left(-\frac{E_a}{RT}\right) \quad (1)$$

$$\ln k_{O_3} = -\frac{E_a}{RT} + \ln A \quad (2)$$

where  $R$ ,  $T$ ,  $E_a$ , and  $A$  are the universal gas constant (8.3145 J K<sup>-1</sup> mol<sup>-1</sup>), absolute temperature (K), activation energy (J mol<sup>-1</sup>), and pre-exponential factor (M<sup>-1</sup> s<sup>-1</sup>), respectively.

The aims of this study were to investigate kinetics, activation energies, and mechanisms for the reactions of ozone with 19 olefins and 3 alkynes. Measurements of  $k_{O_3}$  were performed in the pH range of 1.7–7.0 for olefins and alkynes depending on their chemical structures. A temperature range of 10–25 °C was chosen for the calculation of activation energies. 2-Buten-1,4-dial (BDA, olefin), a problematic transformation product from oxidation of phenols, and 2-ethynylbenzaldehyde (alkyne) were selected for detailed mechanistic studies.

## 2. MATERIALS AND METHODS

**2.1. Chemicals.** Chemicals were mostly obtained from commercial suppliers and used without further purification (for details, see Text S1 (Supporting Information)). Ozone stock solutions were prepared and standardized similarly as in previous studies (Text S2).<sup>24</sup> The hydrolysis of one mol of 2,5-dimethoxy-2,5-dihydrofuran (DMDF) theoretically gives rise to the formation of one mol of BDA with the release of two mols of methanol, where the presence of acid promotes the forward reaction (Scheme S1).<sup>29</sup> Hence, BDA was synthesized from the hydrolysis of DMDF in the presence of polymer-bound *p*-toluenesulfonic acid (TSA) which can be removed by filtration (Text S3 and Figures S1 and S2). This was necessary to avoid oligomerization with the formation of polymers in the presence of a residual acid.

**2.2. Characterization of BDA.** Figure S3 depicts the cross-signals in the <sup>1</sup>H–<sup>13</sup>C heteronuclear single-quantum correlation (HSQC) NMR spectrum, which can be assigned to a mixture of the *cis*- and *trans*-isomers of BDA hydrates, in agreement with previous observations.<sup>30</sup> The relative concentrations of the two isomers can be obtained based on the integrals for the signals of

*cis*- and *trans*-isomers (Figure 1a). The signals of methanol (resonance at 3.34 ppm) and traces of ethanol and tetrahydrofuran (THF) were identified (Figure 1b), for which relative concentrations with respect to BDA hydrates can also be calculated (Text S3). As summarized in Table S1, a stable *cis*-isomer: *trans*-isomer ratio of 56%:44% for the BDA hydrates was obtained for five different batches. The synthesis method developed in this study made it possible to obtain a fast and complete conversion to BDA hydrates without the formation of polymeric products. Identical NMR analysis results for different batches of BDA samples indicate that the hydrolysis protocol is reproducible.

**2.3. Ozone Kinetics.**  $k_{O_3}$  for 19 olefins and 3 alkynes were determined. Among them,  $k_{O_3}$  for 20 compounds were determined by stopped-flow and for 2 compounds also verified by competition kinetics, while for sorbic alcohol and  $\beta$ -cyclocitral, they were only determined by competition kinetics due to the lack of an appropriate UV absorbance, which is necessary for stopped-flow measurements (Table S2). Tertiary butanol (*t*-BuOH) was used in all experiments to scavenge hydroxyl radicals ( $\bullet$ OH).<sup>4</sup> Low pH is favorable to stabilize ozone in aqueous solutions,<sup>4</sup> and therefore, pH 2.3  $\pm$  0.1 (10 mM phosphate buffer) was commonly applied for kinetics measurement, if not otherwise specified.

Stopped-flow experiments were carried out under pseudo-first-order conditions ( $[\text{target compound}]_0 : [\text{O}_3]_0$  (molar ratio)  $\geq 10:1$ ), in the presence of excess *t*-BuOH to scavenge  $\geq 90\%$   $\bullet$ OH by considering the  $k_{OH}$  for the selected compounds (for details of *t*-BuOH concentrations, see Table S3).  $k_{O_3}$  values were measured at 10, 15, 20, and 25 ( $\pm 1$ ) °C to determine activation energies. The apparent second-order rate constants ( $k_{app, O_3}$ ) for olefins and alkynes containing carboxylic acid groups were determined at pH 7.0 and/or other pH (1.7–6.0) to account for the speciation of these compounds. The experimental conditions for each compound are summarized in Table S4. The calculation methods for  $k_{O_3}$  from the evolution of absorbance at the working wavelength in the stopped-flow spectrophotometer are provided in Text S4.

For competition kinetics,<sup>4,26</sup> a series of identical reaction solutions containing the target compound and a competitor mostly in the presence of 0.1 M *t*-BuOH were prepared, followed by addition of variable ozone doses (for details, see Figure S4). For 2-ethynylbenzaldehyde, kinetic experiments were performed at pH 7.0 because  $k_{O_3}$  for the competitor bezafibrate is only available at pH 7.0 in the literature.<sup>26</sup>  $k_{O_3}$  can be calculated from the relative abatement of the target compound (C) and competitor (P) by plotting  $\ln([C]/[C]_0)$  as a function of  $\ln([P]/[P]_0)$  according to eq 3.<sup>4</sup>

$$\ln\left(\frac{[C]}{[C]_0}\right) = \ln\left(\frac{[P]}{[P]_0}\right) \frac{k_{O_3-C}}{k_{O_3-P}} \quad (3)$$

where  $[C]$  and  $[P]$ ,  $[C]_0$  and  $[P]_0$ , and  $k_{O_3-C}$  and  $k_{O_3-P}$  are instant concentrations, initial concentrations, and  $k_{O_3}$  for the target compound C and competitor P, respectively.

All experiments were performed at least in duplicate, and the reported data are average values.

**2.4. Transformation of BDA during Ozonation.** To further investigate the reaction of BDA with ozone, the ensuing formation and yield of glyoxal was determined by derivatization

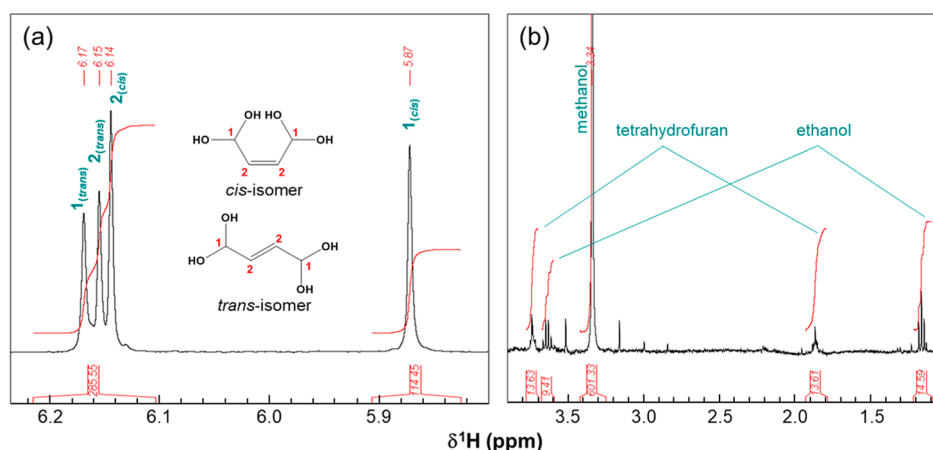


**Figure 1.** Regions of interest of the <sup>1</sup>H NMR spectrum for a 1 mM BDA solution. (a) Resonance assignments and chemical structures of *cis*- and *trans*-BDA hydrates (including integrals) and (b) assignments of signals of methanol (mainly resulting from the hydrolysis of 2,5-dimethoxy-2,5-dihydrofuran) and ethanol and tetrahydrofuran (present as residual solvents in the TSA resin).

with *p*-toluenesulfonyl hydrazide to generate a hydrazone, which can be measured by LC–MS/MS<sup>31,32</sup> or HPLC (for details, see Text S5). Glyoxal is present in the form of a trimer dihydrate in the commercial standard, and therefore, for the preparation of the glyoxal stock solutions, sufficient equilibration time ( $\geq 2$  h, Figure S5) is required for the standard reagent to produce monomer-containing solutions (Scheme S2 and Text S6).

**2.5. Transformation of 2-Ethynylbenzaldehyde during Ozonation.** For the identification of transformation products, 200  $\mu$ M 2-ethynylbenzaldehyde in 10 mM phosphate buffer (pH 2.3) was ozonated with a molar ratio of  $[\text{O}_3]:[2\text{-ethynylbenzaldehyde}] \leq 1:1$  in the presence of 20 mM *t*-BuOH. For the determination of the  $\text{H}_2\text{O}_2$  yield, 500  $\mu$ M 2-ethynylbenzaldehyde in the presence of 10 mM dimethyl sulfoxide (DMSO) instead of *t*-BuOH as a  $\cdot\text{OH}$  scavenger was ozonated to avoid  $\text{H}_2\text{O}_2$  formation from the  $\cdot\text{OH}$  reaction with *t*-BuOH (yield up to 30%<sup>33</sup> but negligible for DMSO<sup>34</sup>). The formation of  $\text{H}_2\text{O}_2$  was quantified by Allen's reagent method to avoid interference from organic peroxides (Text S7 and Figure S6).<sup>35</sup> 2-Carboxybenzaldehyde and phthalaldehyde are identified as transformation products from the ozonation of 2-ethynylbenzaldehyde, with commercially available standards (for details, see below). Their  $k_{\text{O}_3}$  were further measured to clarify the fate of 2-ethynylbenzaldehyde during ozone reaction, by measurements of the ozone decrease (ozone measurement by the indigo method)<sup>36</sup> under pseudo-first-order conditions in excess of the target compounds<sup>25,37</sup> (for details, see Text S8).

**2.6. Analytical Methods.** The synthesized BDA was analyzed by a Bruker AV-III 400 NMR spectrometer (Bruker BioSpin AG, Switzerland).

Kinetics measurements by stopped-flow were performed with an SF-61DX2 stopped-flow instrument (Hitech Scientific), and the data analyses were performed by software installed on the stopped-flow instrument (kinetic studio software).

The measurement of competition kinetics and quantification of glyoxal hydrazone, 2-carboxybenzaldehyde, and 2-ethynylbenzaldehyde were performed by an Ultimate 3000 HPLC-UV (Thermo Scientific).

The identification of transformation products from ozonated 2-ethynylbenzaldehyde was carried out by a Vanquish UHPLC system (Thermo Scientific)-Orbitrap mass analyzer (Orbitrap Exploris 120, Thermo Fisher). More details on the analytical methods are provided in Texts S4 and S9–S11.

### 3. RESULTS AND DISCUSSION

**3.1. Ozone Kinetics.** Cinnamic acid (carboxylic acid group,  $pK_a = 4.44$ ),<sup>38</sup> an olefinic compound with well-known  $k_{\text{O}_3}$ ,<sup>8,39–41</sup> was used to validate the kinetics measurement system applied in this study. The reactivity of olefins with ozone is pH-independent unless adjacent functional groups undergo acid–base speciation. Species-specific second-order rate constants (20  $^{\circ}\text{C}$ ) for cinnamic acid for the neutral and anionic forms were determined as  $(6.9 \pm 0.04) \times 10^4$  and  $(9.0 \pm 0.1) \times 10^5 \text{ M}^{-1} \text{ s}^{-1}$ , respectively (Table 1). They are consistent with the most recently reported values (20  $^{\circ}\text{C}$ ) of  $5.8 \times 10^4$  and  $7.5 \times 10^5 \text{ M}^{-1} \text{ s}^{-1}$ , respectively,<sup>8</sup> as well as a previous  $k_{\text{O}_3}$  at pH 6.5 (22  $^{\circ}\text{C}$ ,  $7.6 \times 10^5 \text{ M}^{-1} \text{ s}^{-1}$ )<sup>24</sup> (Table S5, with a difference of  $<20\%$ ). Based on this data, the pH dependence of  $k_{\text{app},\text{O}_3}$  can be calculated by the fractions of the protonated and deprotonated species and the corresponding species-specific second-order rate constants.<sup>4</sup>

**3.1.1. Second-Order Rate Constants for Reactions of Ozone with Target Olefins.** Different classes of olefins (as outlined in Table 1) were selected to investigate the effects of carbonyl, carboxyl, and alcohol substituents on their reactivity. The target aliphatic olefins were divided into four groups based on their structural characteristics.

**Group 1: Symmetrically Substituted Mono-olefinic Compounds.** A significant dependence of the reactivity on the type of substituent was observed. For example,  $k_{\text{O}_3}$  (20  $^{\circ}\text{C}$ ) for *cis*-2-buten-1,4-diol ( $\text{CH}_2\text{OH}$  substitution) is  $(3.4 \pm 0.1) \times 10^5 \text{ M}^{-1} \text{ s}^{-1}$ , which is 2 orders of magnitude higher than for *cis*-2-buten-1,4-dial (*cis*-BDA,  $\text{CHO}$  substitution,  $(3.0 \pm 0.04) \times 10^3 \text{ M}^{-1} \text{ s}^{-1}$ , Table 1). Since ozone preferentially attacks electron-rich moieties, an electron-withdrawing substituent typically leads to a decreasing reactivity of olefinic compounds. Taft  $\sigma^*$  constants are commonly applied descriptors for inductive effects of substituents.<sup>42</sup> A  $-\text{CH}_2\text{OH}$  group as in *cis*-2-buten-1,4-diol exhibits a lower electron-withdrawing effect than  $-\text{CHO}$  as in *cis*-BDA, with the corresponding Taft  $\sigma^*$  values of 0.62 and 2.15, respectively.<sup>42</sup> A higher ozone reactivity of *cis*-2-buten-1,4-diol compared to that of *cis*-BDA is in line with this concept. For *cis*-1,4-dichloro-2-butene, the  $-\text{CH}_2\text{Cl}$  group has an electron-withdrawing effect ( $\sigma^* = 1.05$ ) between  $-\text{CH}_2\text{OH}$  and  $-\text{CHO}$ , which is reflected in an intermediate  $k_{\text{O}_3}$  ( $(1.9 \pm 0.03) \times 10^4 \text{ M}^{-1} \text{ s}^{-1}$ , Table 1). Different  $k_{\text{app},\text{O}_3}$  values for maleic acid<sup>43–46</sup> and

**Table 1. Determined Second-Order Rate Constants ( $k_{\text{O}_3}$ ) and Activation Energies ( $E_a$ ) for the Reactions of Ozone with Selected Olefins and Alkynes (Groups I–V)**

compound	structure	species-specific second-order rate constant (M <sup>-1</sup> s <sup>-1</sup> ) <sup>b</sup>			k <sub>o</sub> , (M <sup>-1</sup> s <sup>-1</sup> )	pH (± 0.1)	T (°C) <sup>d</sup>	E <sub>a</sub> (kJ mol <sup>-1</sup> ) <sup>e</sup>
		neutral	monoanion	dianion				
reference compound								
cinnamic acid		(6.9 ± 0.04) × 10 <sup>4</sup>	(9.0 ± 0.1) × 10 <sup>5</sup>		(7.5 ± 0.2) × 10 <sup>4</sup> (8.9 ± 0.2) × 10 <sup>5</sup>	2.3 7.0	20 ± 1	25.8 ± 2.6 20.6 ± 0.1
group I: RHC=CHR <sup>c</sup>								
2-buten-1,4-dial <sub>mix</sub> <sup>a</sup>					(7.1 ± 0.1) × 10 <sup>3</sup>	2.3	20 ± 1	30.1 ± 2.3
cis-2-buten-1,4-dial					(3.0 ± 0.04) × 10 <sup>3</sup>	2.3	20 ± 1	
trans-2-buten-1,4-dial					(1.2 ± 0.03) × 10 <sup>4</sup>	2.3	20 ± 1	
cis-2-buten-1,4-diol					(3.4 ± 0.1) × 10 <sup>5</sup>	2.3	20 ± 1	17.4 ± 0.8
cis-1,4-dichloro-2-butene					(1.9 ± 0.03) × 10 <sup>4</sup>	2.3	20 ± 1	31.1 ± 1.8
fumaric acid		(4.9 ± 0.2) × 10 <sup>3</sup>	(2.1 ± 0.04) × 10 <sup>4</sup>	(1.3 ± 0.01) × 10 <sup>5</sup>	(7.6 ± 0.1) × 10 <sup>3</sup>	2.3	20 ± 1	27.3 ± 0.3
					(1.5 ± 0.02) × 10 <sup>4</sup>	3.0		
					(1.3 ± 0.01) × 10 <sup>5</sup>	7.0		
					(9.7 ± 0.1) × 10 <sup>2</sup>	1.7		
					(1.6 ± 0.1) × 10 <sup>3</sup>	2.3		29.3 ± 1.1
maleic acid		(1.5 ± 0.01) × 10 <sup>2</sup>	(2.4 ± 0.02) × 10 <sup>3</sup>	(5.3 ± 0.1) × 10 <sup>3</sup>	(2.2 ± 0.02) × 10 <sup>3</sup>	3.0	20 ± 1	
					(3.7 ± 0.4) × 10 <sup>3</sup>	6.0		
					(4.9 ± 0.01) × 10 <sup>3</sup>	7.0		
					(5.2 ± 0.2) × 10 <sup>3</sup>	7.8		
group II: R <sub>1</sub> R <sub>2</sub> C=CHR <sub>3</sub>								
3-buten-1-ol					(3.6 ± 0.1) × 10 <sup>5</sup>	2.3	20 ± 1	22.0 ± 0.4
3-buten-2-ol					(9.9 ± 0.04) × 10 <sup>4</sup>	2.3	20 ± 1	23.3 ± 0.2
trans-2-methyl-2-butenal					(4.2 ± 0.01) × 10 <sup>4</sup>	2.3	20 ± 1	30.0 ± 0.7
trans-2-pentenal					(1.0 ± 0.1) × 10 <sup>4</sup>	2.3	20 ± 1	37.2 ± 2.8
group III: R <sub>1</sub> HC=CH-CH=CHR <sub>2</sub>								
trans,trans-muconic acid		(6.2 ± 0.5) × 10 <sup>3</sup>	(1.2 ± 0.2) × 10 <sup>4</sup>	(1.7 ± 0.01) × 10 <sup>5</sup>	(8.3 ± 0.2) × 10 <sup>3</sup>	2.3	20 ± 1	23.5 ± 1.4
					(1.2 ± 0.1) × 10 <sup>4</sup>	3.0		
					(1.7 ± 0.01) × 10 <sup>5</sup>	7.0		
sorbic acid		(4.4 ± 0.1) × 10 <sup>5</sup>	(2.0 ± 0.03) × 10 <sup>6</sup>		(4.4 ± 0.1) × 10 <sup>5</sup> (2.0 ± 0.1) × 10 <sup>6</sup>	2.3 7.0	20 ± 1	26.1 ± 2.3
sorbic alcohol					(7.8 ± 0.1) × 10 <sup>5</sup>	2.3	25 ± 2	
sorbic aldehyde					(1.8 ± 0.04) × 10 <sup>5</sup>	2.3	20 ± 1	33.5 ± 3.0
group IV: cyclic olefins								
1-acetyl-1-cyclohexene					(2.0 ± 0.01) × 10 <sup>5</sup>	2.3	20 ± 1	24.5 ± 0.7
β-cyclocitral					(6.8 ± 0.4) × 10 <sup>3</sup>	2.3	20 ± 2	
2-cyclopenten-1-one					(4.2 ± 0.1) × 10 <sup>3</sup>	2.3	20 ± 1	32.4 ± 0.8
4-cyclopentene-1,3-dione					(2.3 ± 0.1) × 10 <sup>2</sup>	2.3	20 ± 1	37.7 ± 0.1
group V: alkynes								
3-butyne-1-ol					(4.9 ± 0.2) × 10 <sup>2</sup>	2.3	20 ± 1	36.7 ± 0.8
3-butyric acid		(1.8 ± 0.1) × 10 <sup>2</sup>	(6.2 ± 0.2) × 10 <sup>2</sup>		(2.0 ± 0.1) × 10 <sup>2</sup>	2.3	20 ± 1	42.0 ± 0.3
					(6.2 ± 0.4) × 10 <sup>2</sup>	7.0		
2-ethynylbenzaldehyde					(1.6 ± 0.03) × 10 <sup>2</sup>	2.3	20 ± 1	48.1 ± 4.2

<sup>a</sup>2-Buten-1,4-dial<sub>mix</sub>: mixture of 56% *cis*- and 44% *trans*-isomers (results for the fractions are shown in Table S1), both present in the form of hydrates in aqueous solution. <sup>b</sup>Calculated from the determined  $k_{\text{app},\text{O}_3}$  values at different pHs. <sup>c</sup>R: Substituents of olefins. <sup>d</sup>T: Temperature for the present  $k_{\text{O}_3}$  determination, which was the same for selected compounds at different pHs. <sup>e</sup> $E_a$  values for cinnamic acid were determined at pH 2.3 ( $25.8 \pm 2.6 \text{ kJ mol}^{-1}$ ) and 7.0 ( $20.6 \pm 0.1 \text{ kJ mol}^{-1}$ ); for all other compounds, they were determined at pH 2.3.

fumaric acid<sup>43,46,47</sup> were reported in the literature (Table S5). The obtained  $k_{\text{app},\text{O}_3}$  values (20  $^{\circ}\text{C}$ ) for maleic acid of  $(1.3 \pm 0.01) \times 10^3$  (calculated, pH 2.0),  $(3.7 \pm 0.4) \times 10^3$  (pH 6.0,

Table 1), and  $(4.9 \pm 0.01) \times 10^3 \text{ M}^{-1} \text{ s}^{-1}$  (pH 7.0, Table 1) and for fumaric acid of  $(6.3 \pm 0.1) \times 10^3$  (calculated, pH 2.0),  $(1.1 \pm 0.01) \times 10^5$  (calculated, pH 5.0), and  $(1.3 \pm 0.01) \times 10^5 \text{ M}^{-1} \text{ s}^{-1}$  (pH 7.0, Table 1) differ by less than a factor of 2 from most



previously reported values<sup>43,47</sup> and calculated values from the reported species-specific second-order rate constants (Table S5).<sup>46</sup> Their species-specific second-order rate constants follow the order of dianion > monoanion > acid, consistent with the expected induction effect of the carboxylic acid group.<sup>48,49</sup> Figure S7 shows the measured and calculated pH dependence of the  $k_{\text{app},\text{O}_3}$  values of maleic acid. The good agreement between the experiments and calculations confirms the validity of this approach. Maleic acid and fumaric acid are stereoisomers (*cis* and *trans*, respectively), but fumaric acid is 1 order of magnitude more reactive than maleic acid. A similar phenomenon was also observed for 1,2-dichloroethene<sup>25,27</sup> and 1,1,3,4-tetrachloro-1,3-butadiene<sup>50</sup> (Table S5). This could be partially explained by the *cis* effect, an observation that the *cis*-isomer is more stable than the corresponding *trans*-isomer.<sup>51,52</sup> In the case of monoanions, the lower reactivity of maleic acid compared to fumaric acid could be due to the generation of intramolecular hydrogen bonds promoting its stability.<sup>53</sup>

**Group II. Asymmetrically Substituted Mono-olefinic Compounds.** The determined  $k_{\text{O}_3}$  values at 20 °C for group II compounds are in the range of  $10^4$ – $10^5$   $\text{M}^{-1} \text{s}^{-1}$ .  $k_{\text{O}_3}$  for *trans*-2-methyl-2-butenal ( $(4.2 \pm 0.01) \times 10^4$   $\text{M}^{-1} \text{s}^{-1}$ , Table 1) differed by a factor of 2 compared to the reported value for methacrolein ( $1.9 \times 10^4$   $\text{M}^{-1} \text{s}^{-1}$ ,<sup>54</sup> Table S5). This was attributed to an additional  $-\text{CH}_3$  group at the olefin in *trans*-2-methyl-2-butenal, which leads to a higher electron density.  $k_{\text{O}_3}$  for methacrolein<sup>54</sup> (Table S5) was nearly a factor of 2 higher than for *trans*-2-pentenal ( $(1.0 \pm 0.1) \times 10^4$   $\text{M}^{-1} \text{s}^{-1}$ , Table 1). This is likely due to the  $\alpha$  position of the  $-\text{CH}_3$  group for methacrolein compared to the  $-\text{CH}_2\text{CH}_3$  group in the  $\beta$  position for *trans*-2-pentenal. Other evidence for the effect of positions of substituents on the compound's reactivities is provided by comparing 3-buten-1-ol and 3-buten-2-ol. The distance of the electron-withdrawing  $-\text{OH}$  group from the double bond decreases in the order of 3-buten-1-ol > 3-buten-2-ol, which is reflected in a consistent trend of  $k_{\text{O}_3}$  being  $(3.6 \pm 0.1) \times 10^5$   $\text{M}^{-1} \text{s}^{-1}$  (Table 1) and  $(9.9 \pm 0.04) \times 10^4$   $\text{M}^{-1} \text{s}^{-1}$  (Table 1; previously reported values  $7.9 \times 10^{427}$  and  $9.1 \times 10^4$   $\text{M}^{-1} \text{s}^{-1}$ ,<sup>55</sup> Table S5), respectively.

**Group III: Olefins with Conjugated Double Bonds.** *trans*-, *trans*-muconic acid was used as a representative compound of this group, and the stoichiometry for the ozone reaction was demonstrated to be 1 for molar ratios of ozone:*trans*-, *trans*-muconic acid < 1 (Figure S8). Since there are two olefinic groups, the second double bond also reacts in excess of ozone. Muconic acid exists in three stereoisomers: *trans*-, *trans*-muconic acid, *cis*-, *trans*-muconic acid, and *cis*-, *cis*-muconic acid. Unfortunately, the species-specific second-order rate constants for the *cis*-, *trans*- and *cis*-, *cis*-isomers are unavailable, and therefore, a comparison of ozone reactivities for the respective species of the three isomers is impossible. For *trans*-, *trans*-muconic acid, which has carboxylic acid groups at both ends, its species-specific second-order rate constants are about 1–2 orders of magnitude lower than those of sorbic acid, which has a  $-\text{CH}_3$  group at one end instead (Table 1). This difference is consistent with the electron-withdrawing effect of the carboxylic acid group compared with the electron-donating effect of the  $-\text{CH}_3$  group. Sorbic alcohol, sorbic acid, and sorbic aldehyde have the same structural features with  $\text{H}_3\text{C}-\text{CH}=\text{CH}-\text{CH}=\text{CH}-\text{R}$ , where R is  $-\text{CH}_2\text{OH}$ ,  $-\text{COOH}$ , and  $-\text{CHO}$ , with  $k_{\text{O}_3}$  at pH 2.3 (25 °C) being  $(7.8 \pm 0.1) \times 10^5$  (Table 1),  $(5.2 \pm 0.04) \times 10^5$  (Table S4), and  $(2.2 \pm 0.1) \times 10^5$   $\text{M}^{-1} \text{s}^{-1}$  (Table S4),

respectively. These reactivities are in line with the electron-withdrawing effects of the substituents R which increase in the order of  $-\text{CH}_2\text{OH}$  (Taft  $\sigma^* = 0.62$ ) <  $-\text{COOH}$  (2.08) <  $-\text{CHO}$  (2.15). The  $k_{\text{app},\text{O}_3}$  for sorbic acid at pH 3.0 and 8.0 were previously reported to be  $3.2 \times 10^5$  and  $9.6 \times 10^5$   $\text{M}^{-1} \text{s}^{-1}$  (Table S5),<sup>56</sup> respectively, using an earlier published  $k_{\text{app},\text{O}_3}$  for cinnamic acid as a competitor.<sup>39</sup> After correction with  $k_{\text{app},\text{O}_3}$  values for cinnamic acid determined in this study (Table 1), the  $k_{\text{app},\text{O}_3}$  for sorbic acid at pH 3.0 and 8.0 could be updated to  $4.8 \times 10^5$  and  $2.3 \times 10^6$   $\text{M}^{-1} \text{s}^{-1}$ , respectively. This is very close to the  $k_{\text{app},\text{O}_3}$  values at pH 3 and 8 obtained in the current study being  $(4.7 \pm 0.1) \times 10^5$  and  $(2.0 \pm 0.03) \times 10^6$   $\text{M}^{-1} \text{s}^{-1}$ , respectively (calculated from the determined species-specific second-order rate constants for sorbic acid, Table 1).

**Group IV: Cyclic Olefins.** There is only limited information on the reactivities of this class of compounds.<sup>9,57,58</sup> As for the open-chain olefins, substituents in the  $\alpha$  position have a pronounced effect on the ozone reactivities. Cyclohexene ( $2.2 \times 10^6$   $\text{M}^{-1} \text{s}^{-1}$  at 25 °C,<sup>57</sup> Table S5) is about 1 order of magnitude more reactive than 1-acetyl-1-cyclohexene ( $(2.3 \pm 0.04) \times 10^5$   $\text{M}^{-1} \text{s}^{-1}$  at 25 °C, Table S4), attributed to the electron-withdrawing effect of the  $-\text{CO}-\text{CH}_3$  group on the latter. 2-Cyclopenten-1-one and 4-cyclopenten-1,3-dione with one and two carbonyl groups in the  $\alpha$  position, respectively, differ in their reactivities with ozone by about 1 order of magnitude, with  $k_{\text{O}_3} = (4.2 \pm 0.1) \times 10^3$  and  $(2.3 \pm 0.1) \times 10^2$   $\text{M}^{-1} \text{s}^{-1}$ , respectively (20 °C, Table 1). As shown in Table S6, cyclohexene, 1-acetyl-1-cyclohexene, and  $\beta$ -cyclocitral contain the basic olefinic structures of ethene, methyl vinyl ketone, and 2-butenal, respectively. Relative to ethene ( $1.8 \times 10^5$   $\text{M}^{-1} \text{s}^{-1}$ )<sup>27</sup> and methyl vinyl ketone ( $3.7 \times 10^4$   $\text{M}^{-1} \text{s}^{-1}$ ),<sup>54</sup> the  $k_{\text{O}_3}$  values of cyclohexene ( $2.2 \times 10^6$   $\text{M}^{-1} \text{s}^{-1}$ )<sup>57</sup> and 1-acetyl-1-cyclohexene ( $(2.0 \pm 0.01) \times 10^5$   $\text{M}^{-1} \text{s}^{-1}$ , this study) are higher by factors of 12 and 5, respectively. This is likely due to the electron-donating effect of the adjacent alkyl groups in the case of the ring structures. However, relative to 2-butenal ( $k_{\text{O}_3}$  not measured but approximated by *trans*-2-methyl-2-butenal,  $(4.2 \pm 0.01) \times 10^4$   $\text{M}^{-1} \text{s}^{-1}$ ), the  $k_{\text{O}_3}$  for  $\beta$ -cyclocitral ( $(6.8 \pm 0.4) \times 10^3$   $\text{M}^{-1} \text{s}^{-1}$ , Table 1; previously reported value  $3.9 \times 10^3$   $\text{M}^{-1} \text{s}^{-1}$ ,<sup>9</sup> Table S5) is lower by a factor of 6–11. The large difference in  $k_{\text{O}_3}$  is possibly caused by the steric hindrance of an ozone attack on the ring structure of  $\beta$ -cyclocitral. A 4 orders of magnitude decrease in  $k_{\text{O}_3}$  caused by the steric effect has been observed for endrin ( $< 2.0 \times 10^{-2}$   $\text{M}^{-1} \text{s}^{-1}$ ,<sup>37</sup> Table S5) compared to *cis*-, 1,2-dichloroethene ( $(3.1-8.0) \times 10^2$   $\text{M}^{-1} \text{s}^{-1}$ ,<sup>25,27,37</sup> Table S5).

The electronic effects discussed above for noncyclic olefins (groups I–III) also apply to heterocyclic olefins (Table S7). Addition of electron-donating groups ( $-\text{CH}_3$ ) to the carbon-carbon double bond as in 4-methylimidazole (protonated,  $1.7 \times 10^3$   $\text{M}^{-1} \text{s}^{-1}$ )<sup>45</sup> increases the  $k_{\text{O}_3}$  compared to imidazole (protonated,  $2.2 \times 10^1$   $\text{M}^{-1} \text{s}^{-1}$ <sup>143</sup>– $1.5 \times 10^3$   $\text{M}^{-1} \text{s}^{-1}$ <sup>159</sup>). Conversely, the addition of electron-withdrawing  $-\text{CO}$  groups in maleimide ( $4.2 \times 10^3$   $\text{M}^{-1} \text{s}^{-1}$ )<sup>59</sup> significantly decreases the  $k_{\text{O}_3}$  when compared to pyrrole ( $8.6 \times 10^5$   $\text{M}^{-1} \text{s}^{-1}$ ).<sup>59</sup> A similar pattern was observed for furans. At pH 7, the degree of electron withdrawal by the carboxylic acid group attached to the furan ring, with  $-\text{COO}^-$  as the predominant form because of a  $\text{p}K_a < 4.4$ ,<sup>60,61</sup> follows this sequence: 3-(2-furyl) propanoic acid < 2-furoic acid < furan-2,5-dicarboxylic acid, and consequently, the

$k_{\text{app},\text{O}_3}$  values show the opposite tendency ( $3.2 \times 10^6$ ,  $5.9 \times 10^5$ , and  $8.5 \times 10^4 \text{ M}^{-1} \text{ s}^{-1}$ , respectively, Table S7).<sup>62</sup>

Taft  $\sigma^*$  constants have been previously applied to develop quantitative structure–activity relationships (QSAR) for predicting  $k_{\text{O}_3}$  of organic compounds containing ozone-reactive functional groups such as olefins.<sup>63</sup> However, Taft  $\sigma^*$  constants are not always available; for instance, the values for groups like  $-\text{CH}=\text{CH}-\text{CH}_2\text{OH}$  in sorbic alcohol and for cyclic structures remain undefined. Moreover, Taft  $\sigma^*$  constants have limitations, such as their inability to distinguish stereoisomers (e.g., maleic acid and fumaric acid, which share identical Taft  $\sigma^*$  constants despite their distinct stereochemistry). These constraints hindered the development of a comprehensive QSAR model to all the measured olefins in this study.

**3.1.2. Second-Order Rate Constants for Reactions of Ozone with Target Alkynes.**  $k_{\text{O}_3}$  values for the three selected alkynes at 20 °C were determined to be in the range of  $(1.6 \pm 0.03) \times 10^2$ – $(6.2 \pm 0.4) \times 10^2 \text{ M}^{-1} \text{ s}^{-1}$  (Table 1). This is similar to reported  $k_{\text{O}_3}$  for 1-ethynyl-1-cyclohexanol ( $2 \times 10^2 \text{ M}^{-1} \text{ s}^{-1}$ ,<sup>16</sup> Table S5).  $k_{\text{O}_3}$  values for the reactions of ozone with alkynes ( $\sim 10^2 \text{ M}^{-1} \text{ s}^{-1}$ ) are significantly lower than those for olefins (mostly  $10^3$ – $10^6 \text{ M}^{-1} \text{ s}^{-1}$ , see above). For 3-butyne-1-ol as a representative alkyne,  $k_{\text{O}_3}$  is  $(4.9 \pm 0.2) \times 10^2 \text{ M}^{-1} \text{ s}^{-1}$  (Table 1), which is 3 orders of magnitude lower than for the corresponding olefin 3-buten-1-ol ( $(3.6 \pm 0.1) \times 10^5 \text{ M}^{-1} \text{ s}^{-1}$ , Table 1). It may be surprising to observe this pattern because the electron density in alkynes is also high. One possible explanation could be the stronger  $\pi$  bonds in alkynes than olefins, as reflected by the shorter carbon–carbon triple bond length compared to carbon–carbon double bond length,<sup>64</sup> which has been verified by calculations using acetylene and ethene as examples.<sup>65</sup> Because of an acid–base speciation of 3-butyneic acid ( $\text{p}K_{\text{a}} = 3.62$ ,<sup>66</sup> predicted), the species-specific second-order rate constants (20 °C) were determined to be  $(1.8 \pm 0.1) \times 10^2$  and  $(6.2 \pm 0.2) \times 10^2 \text{ M}^{-1} \text{ s}^{-1}$  for the protonated and deprotonated forms, respectively (Table 1). The effect of substituents on the alkyne reactivity was tested and  $k_{\text{O}_3}$  increased in the order of 3-butyneic acid (acid,  $(1.8 \pm 0.1) \times 10^2 \text{ M}^{-1} \text{ s}^{-1}$ ) < 3-butyne-1-ol ( $(4.9 \pm 0.2) \times 10^2 \text{ M}^{-1} \text{ s}^{-1}$ ) (Table 1). This is consistent with the electron-withdrawing effect of the substituents:  $-\text{COOH}$  (Taft  $\sigma^* = 2.08$ ) >  $-\text{CH}_2\text{OH}$  (0.62).<sup>42</sup> In the case of 1-ethynyl-1-cyclohexanol, the  $-\text{OH}$  group was assumed to show a higher inductive effect than that of the six-membered ring. The  $-\text{OH}$  group of 1-ethynyl-1-cyclohexanol ( $k_{\text{O}_3} = 2 \times 10^2 \text{ M}^{-1} \text{ s}^{-1}$ ,<sup>16</sup> Table S5) was closer to the alkyne group than for 3-butyne-1-ol ( $k_{\text{O}_3} = (4.9 \pm 0.2) \times 10^2 \text{ M}^{-1} \text{ s}^{-1}$ , Table 1), resulting in a higher electron-withdrawing effect with an ensuing lower reactivity with ozone.

**3.2. Activation Energies for Reactions of Ozone with Olefins and Alkynes.** Changes in temperature affect not only second-order rate constants but also the speciation of compounds with acidic functional groups. For cinnamic acid as an example, according to the linear form of the van't Hoff equation (eq 4),<sup>67</sup> its  $\text{p}K_{\text{a}}$  at 10 °C was calculated to be 4.63 after plotting the  $\ln(K_{\text{a}})$  against  $1/T$  in the temperature range of 15–25 °C reported previously (respective  $\text{p}K_{\text{a}} = 4.59$ , 4.53, and 4.50 at 15, 20, and 25 °C).<sup>68</sup>

$$\ln(K_{\text{a}}) = -\frac{\Delta_{\text{r}}H^{\circ}}{RT} + \frac{\Delta_{\text{r}}S^{\circ}}{R} \quad (4)$$

where  $\Delta_{\text{r}}H^{\circ}$  and  $\Delta_{\text{r}}S^{\circ}$  are the standard reaction enthalpy ( $\text{J mol}^{-1}$ ) and standard reaction entropy ( $\text{J K}^{-1} \text{ mol}^{-1}$ ), respectively.

The species distribution of cinnamic acid at pH 2.3 was calculated to be constant with a proportion of the neutral form ranging from 0.995 to 0.993, as the temperature changed from 10 to 25 °C. In this case,  $k_{\text{app},\text{O}_3}$  of cinnamic acid at pH 2.3 gradually increased from  $(5.2 \pm 0.1) \times 10^4 \text{ M}^{-1} \text{ s}^{-1}$  at 10 °C to  $(9.0 \pm 0.8) \times 10^4 \text{ M}^{-1} \text{ s}^{-1}$  at 25 °C (Table S4) and the effect of  $\text{p}K_{\text{a}}$  change can be neglected.

Based on this, a correlation between  $\ln k_{\text{O}_3}$  and the inverse of absolute temperature can be made to obtain the activation energy (eq 2). The activation energy was calculated as  $25.8 \pm 2.6 \text{ kJ mol}^{-1}$  for the ozone reaction with cinnamic acid (Figure S9). Since pH affects the  $k_{\text{app},\text{O}_3}$  for olefins with substituents with acid–base speciation, the activation energy for cinnamic acid was also determined at pH 7.0 to be  $20.6 \pm 0.1 \text{ kJ mol}^{-1}$  (Table 1), which is in agreement with the reported values of  $21.2 \text{ kJ mol}^{-1}$  at pH 6.5<sup>24</sup> and  $19.1 \text{ kJ mol}^{-1}$  at pH 7.2<sup>8</sup> (Table S5). This indicates that changes in the acid–base speciation do affect not only the  $k_{\text{app},\text{O}_3}$  but also the activation energies.

Table 1 reports the activation energies for ozone reactions with selected olefins and alkynes. The minimum and maximum activation energies for the reactions of ozone with olefins were determined to be  $17.4 \pm 0.8 \text{ kJ mol}^{-1}$  for *cis*-2-buten-1,4-diol and  $37.7 \pm 0.1 \text{ kJ mol}^{-1}$  for 4-cyclopenten-1,3-dione, respectively. These results are consistent with previously reported activation energies for ozone reactions with olefins ( $18.0$ – $35.1 \text{ kJ mol}^{-1}$ , Table S5). Overall,  $k_{\text{O}_3}$  values for olefins at 25 °C are about a factor of 1.4–2.3 higher than at 10 °C. The activation energies for the ozone reactions with alkynes are significantly higher than for olefins and ranged from  $36.7$  to  $48.1 \text{ kJ mol}^{-1}$ .  $k_{\text{O}_3}$  values for alkynes at 25 °C are about a factor of 2.2–2.8 higher than at 10 °C.

The activation energies for olefinic compounds determined in this and previous studies were plotted as a function of the logarithm of  $k_{\text{O}_3}$  (Figure S10). There is a moderate correlation between  $k_{\text{O}_3}$  and the activation energy. For most of the selected olefins in this study, activation energies are within a 95% confidence interval of literature-reported  $k_{\text{O}_3}$ . Overall, an order of magnitude increase in  $k_{\text{O}_3}$  was observed for a decrease in the activation energy of about  $5 \text{ kJ mol}^{-1}$ .

To gain more insights into the variations in ozonation efficacy pertaining to the inactivation of microorganisms and oxidation of organic compounds at different temperatures, the effects of temperature (5 and 25 °C) on ozone exposure, the abatement of 2-cyclopenten-1-one and 2-ethynylbenzaldehyde, and the inactivation of *B. subtilis* spores<sup>23</sup> were modeled for ozonation of Lake Zurich water<sup>21</sup> (Text S12 and Figure 2). Figure 2a shows the cumulative ozone exposure as a function of reaction time. Ozone is much less stable at 25 °C, with first-order rate constants for its decrease in the initial and secondary phases of  $5.2 \times 10^{-3} \text{ s}^{-1}$  and  $4.4 \times 10^{-3} \text{ s}^{-1}$ , respectively, compared to 5 °C ( $1.9 \times 10^{-3} \text{ s}^{-1}$  and  $6.0 \times 10^{-4} \text{ s}^{-1}$ , respectively),<sup>21</sup> with an ensuing lower ozone exposure at 25 °C (maximum:  $4.5 \times 10^{-3} \text{ Ms}$ ) than at 5 °C (maximum:  $2.3 \times 10^{-2} \text{ Ms}$ ). Nevertheless, the abatement of 2-cyclopenten-1-one at both temperatures is quite similar. This is due to the offsetting effect of reduced ozone exposure at higher temperature by the increase of  $k_{\text{O}_3}$  of 2-cyclopenten-1-one under these conditions. For 2-ethynylben-

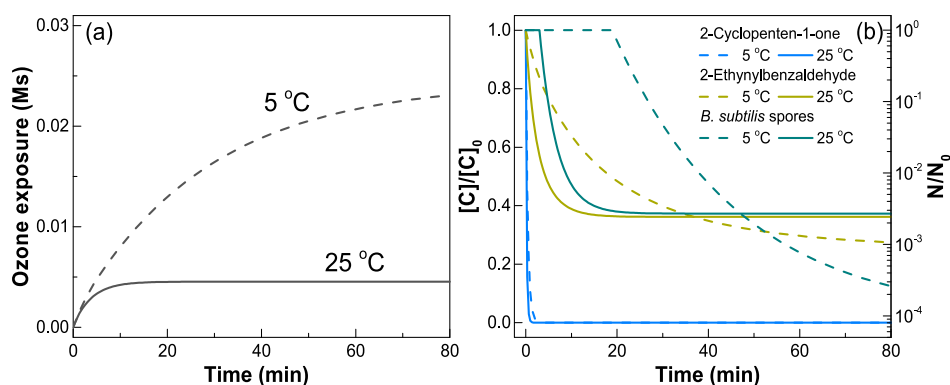


**Figure 2.** Calculated effects of temperature (5 and 25 °C) on (a) ozone exposure and (b) abatement of 2-cyclopenten-1-one and 2-ethynylbenzaldehyde and the inactivation of *B. subtilis* spores in Lake Zurich water.  $[C]/[C]_0$  represents the relative residual concentration of the target compound during ozonation, and  $N/N_0$  represents the relative residual numbers of *B. subtilis* spores during ozonation. Calculation conditions:  $[O_3]_0 = 1 \text{ mg L}^{-1}$ . Detailed kinetic information for the ozone decay, the abatement of 2-cyclopenten-1-one and 2-ethynylbenzaldehyde, and the inactivation of *B. subtilis* spores, as well as the calculation methods are provided in Text S12.

zaldehyde with a much lower  $k_{O_3}$  ( $(2.2 \pm 0.01) \times 10^2 \text{ M}^{-1} \text{ s}^{-1}$  at 25 °C, this study, Table S4), the relative abatement is better at lower temperature for residence times >37 min. The calculated inactivation of *B. subtilis* spores is more efficient at higher temperatures, achieving 2-log inactivation for a contact time of 9 min at 25 °C and 38 min at 5 °C, respectively. This is mainly due to the increased lag phase at lower temperatures, which for higher ozone exposures is no longer critical anymore. However, due to the higher ozone exposure at 5 °C, the inactivation of *B. subtilis* spores continuously proceeded, yielding 3-log inactivation for a contact time of 57 min. Overall, this shows that the water temperature has a significant influence on the efficiency of ozonation processes. For target compounds with intermediate-high  $k_{O_3}$ , the efficiency is similar or better at the higher temperature (e.g., olefins), whereas for slowly reacting targets, the trend may be reversed (e.g., alkynes). For the inactivation of microorganisms, both the inactivation rate constants and a potential lag phase are decisive. The simulation does not provide exact transformation/inactivation data but rather trends, which illustrate the importance of considering temperature changes when going from the laboratory to realistic systems.

### 3.3. Transformation of BDA during Ozonation.

Oxidative treatments (e.g., chlorination, UV photolysis, and radical oxidation) of phenolic compounds can lead to the formation of BDA,<sup>69,70</sup> which is problematic due to the potential genotoxicity and mutagenicity of  $\alpha,\beta$ -unsaturated carbonyls.<sup>15</sup> Even though this compound may be (partially) abated in biological processes,<sup>31</sup> its reactivity with ozone is still of great interest. The lack of a commercial standard makes it difficult to obtain mechanistic information about BDA transformation during ozonation. Hence, BDA was synthesized and characterized (see details in Sections 2.1 and 2.2) before its abatement kinetics and mechanisms were investigated.

**3.3.1. Kinetics of BDA Oxidation by Ozone.** As discussed above, both *cis*- and *trans*-isomers of BDA hydrates are present in the final BDA samples (Figure 1). To gain insights about the reactivities of the two isomers, two batches of kinetic experiments were conducted, as described in Text S13. For the first batch, a  $k_{O_3}$  of  $(7.1 \pm 0.1) \times 10^3 \text{ M}^{-1} \text{ s}^{-1}$  was obtained from the original BDA solution, containing 56% *cis*- and 44% *trans*-BDA. For the second batch, a preozonated BDA sample was prepared with a molar BDA:ozone ratio of 2:1. A  $k_{O_3}$  of  $(4.1$

$\pm 0.1) \times 10^3 \text{ M}^{-1} \text{ s}^{-1}$  was obtained from the preozonated BDA solution (containing a calculated fraction of 88% *cis*- and 12% *trans*-BDA). On the basis of the different fractions of the *cis*- and *trans*-isomers during two batches of  $k_{O_3}$  measurements, individual  $k_{O_3}$  values can be calculated. Considering the *cis* effect (see above),<sup>51,52</sup>  $k_{O_3}$  for the *cis*- and *trans*-isomers were calculated to be  $(3.0 \pm 0.04) \times 10^3$  and  $(1.2 \pm 0.03) \times 10^4 \text{ M}^{-1} \text{ s}^{-1}$ , respectively (Text S13).

**3.3.2. Glyoxal Formation during Ozonation of BDA.** Ozone typically reacts with olefins by the Criegee mechanism.<sup>1</sup> The corresponding transformation pathway for the *cis*- and *trans*-BDA hydrates is shown in Figure 3a. The ozonide (2) formed from the cycloaddition of ozone to BDA decomposes to form one mol of glyoxal (7) and one mol of a zwitterion (4) and the hydrated zwitterion (6) decomposes to another mol of glyoxal ( $6 \rightleftharpoons 5 \rightleftharpoons 7$ ). Overall, two mols of glyoxal are expected to be formed per mol of ozonated BDA. The glyoxal yield as a function of the time increases gradually within 25 h (Figure 3b). At 25 h contact time, 1.84 mol of glyoxal per mol of dosed ozone was determined, which is close to the theoretical factor of 2. Due to uncertainties in ozone dosing, an estimated error of 10% in terms of the glyoxal yield is possible. Under the applied experimental conditions, ozone is completely depleted within 1 min because  $k_{O_3}$  for both *cis*- and *trans*-isomers of BDA hydrates are  $>10^3 \text{ M}^{-1} \text{ s}^{-1}$  (see above). The reversible reactions between the glyoxal trimer and hydrated monomer during preparation of the glyoxal stock solution can also be a potential source of error (Text S6). A similar pattern of glyoxal formation as a function of holding time was also observed when the BDA solution was prepared differently (Figure S11). One mol of glyoxal per mol of consumed BDA was formed relatively fast within about 1 h, which can be interpreted by the decomposition of the Criegee ozonide ( $2 \rightarrow 5$ , Figure 3a). The formation of the second mol of glyoxal takes about 24 h, which can be explained by the decomposition of a relatively stable  $\alpha$ -hydroxyalkylhydroperoxide.<sup>71</sup>

**3.4. Transformation of 2-Ethynylbenzaldehyde during Ozonation.** **3.4.1. Kinetics of the Reaction of Ozone with 2-Ethynylbenzaldehyde.** Figure 4a shows a linear correlation of the abatement of 2-ethynylbenzaldehyde as a function of the ozone dose with a slope = 0.94, indicating a reaction stoichiometry close to 1. As discussed above, the  $k_{O_3}$  values for



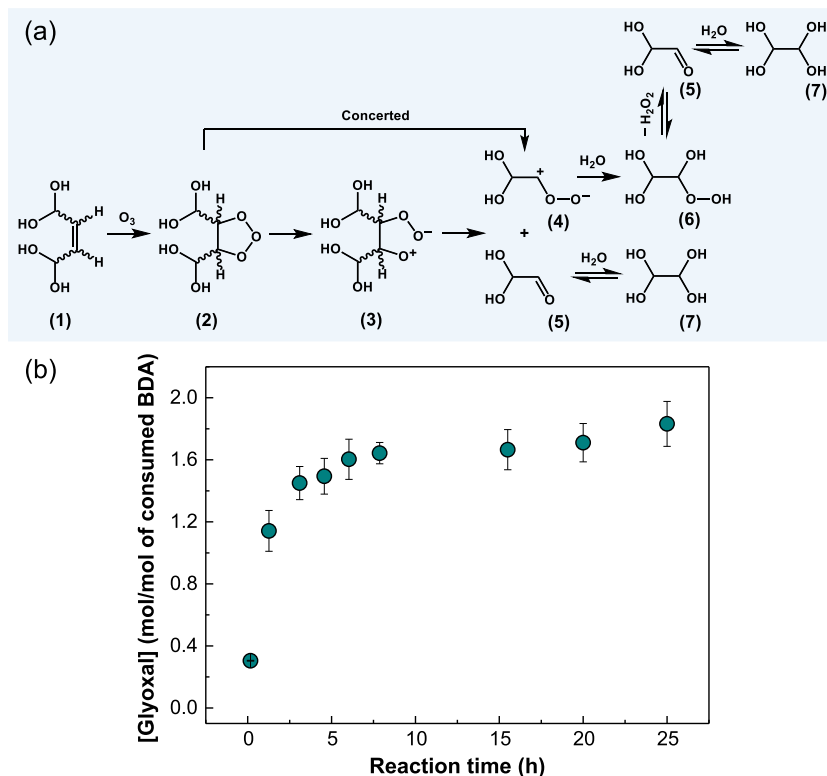


**Figure 3.** Glyoxal formation during ozonation of BDA. (a) General Criegee-type mechanism for the reaction of ozone with the *cis*- and *trans*-isomers of BDA. The wavy bonds stand for the two possible stereoisomers. (b) Glyoxal formation as a function of time after complete depletion of ozone (<1 min). Experimental conditions: [BDA]<sub>0</sub> = 30 μM, [O<sub>3</sub>]<sub>0</sub> = 6 and 12 μM for two experiments, [*t*-BuOH]<sub>0</sub> = 3 mM, pH 2.3, 10 mM phosphate buffer. The BDA was synthesized following the procedure described in Text S3. The circles represent the average values, and the error bars represent the range of the measured values for the two ozone doses.

aliphatic alkynes are on the order of  $10^2 \text{ M}^{-1} \text{ s}^{-1}$ . For 2-ethynylbenzaldehyde,  $k_{\text{O}_3}$  (25 °C, stopped-flow) of  $(2.2 \pm 0.01) \times 10^2 \text{ M}^{-1} \text{ s}^{-1}$  (Table S4) and an activation energy of  $48.1 \pm 4.2 \text{ kJ mol}^{-1}$  (Table 1) have been determined. The reactivity of the compound was further examined through competition kinetics using bezafibrate as a competitor, resulting in a  $k_{\text{O}_3}$  of  $(2.0 \pm 0.1) \times 10^2 \text{ M}^{-1} \text{ s}^{-1}$  ( $25 \pm 2$  °C, Figure S4d), consistent with the value determined via the stopped-flow method. The reactivity of the benzaldehyde component can be disregarded, as it reportedly reacts only slowly with ozone ( $2.5 \text{ M}^{-1} \text{ s}^{-1}$ ).<sup>25</sup> Based on these observations, it can be assumed that for 2-ethynylbenzaldehyde, the ozone attack occurs primarily at the ethynyl group, as expected.

**3.4.2. Determination of Transformation Products from the Reaction of Ozone with 2-Ethynylbenzaldehyde.** Figure 4b shows the proposed transformation pathway for the ozone attack at the ethynyl group of 2-ethynylbenzaldehyde. Ozonation of alkynes is generally assumed to occur similarly to a Criegee-type mechanism.<sup>17</sup> The first step is a cycloaddition to generate an ozonide (9) which further decomposes to the zwitterions (10a and/or 10b). Subsequently, the alkoxyalkyl hydroperoxides (11a and/or 11b) are potentially formed via hydrolysis reactions. Three transformation products with *m/z* of 150 (TP 150), 162 (TP 162), and 134 (TP 134), respectively, were identified using an Orbitrap LC–MS/MS (Text S14). The chemical structure of TP 150 (Figure S12a) and TP 134 (Figure S12b) was confirmed via comparison with commercial standards of 2-carboxybenzaldehyde (Figure S12e) and phthalaldehyde (Figure S12f), respectively. TP 162, despite the lack of a standard, was proposed as a dicarbonyl compound based on the

MS<sup>2</sup> spectrum obtained in the positive ionization mode (Figure S12c), the formation of which occurred with a release of H<sub>2</sub>O<sub>2</sub>. Upon ozonation of 1-ethynyl-1-cyclohexanol, the formation of a corresponding dicarbonyl compound and carboxylic acid compound was also observed previously.<sup>16</sup>

As shown in Figure 4c, the yield of 2-carboxybenzaldehyde (TP 150) was determined to be 54% with respect to the abated 2-ethynylbenzaldehyde. Quantification of phthalaldehyde (TP 134) was not possible due to the low sensitivity of the HPLC analytical method for this compound. For H<sub>2</sub>O<sub>2</sub> quantification, 20 times molar excess of DMSO was used (no H<sub>2</sub>O<sub>2</sub> formation in contrast to *t*-BuOH).<sup>33</sup> Due to its much higher  $k_{\text{O}_3}$  (most recently reported value of  $4.8 \text{ M}^{-1} \text{ s}^{-1}$ )<sup>72</sup> compared to *t*-BuOH ( $0.003 \text{ M}^{-1} \text{ s}^{-1}$ ),<sup>25</sup> DMSO competed for ozone with 2-ethynylbenzaldehyde, with the ozone consumption calculated to be 38% and ensuing 62% by 2-ethynylbenzaldehyde. Consistently, 0.57 mol of 2-ethynylbenzaldehyde was abated per mole of ozone (Figure S13a). Meanwhile, 0.54 mol of 2-carboxybenzaldehyde was detected per mol of consumed 2-ethynylbenzaldehyde (Figure S13b) which is the same as in Figure 4c and indicates that the change of the scavenger did not affect the transformation mechanism. An average H<sub>2</sub>O<sub>2</sub> yield of 21% based on the transformed 2-ethynylbenzaldehyde over the entire ozonation time from 1 to 75 h (Figure S13c) was determined (Figure 4c). Since one mol of H<sub>2</sub>O<sub>2</sub> is released per mol of TP 162 formed, its yield is assumed to be 21% based on the abated 2-ethynylbenzaldehyde. Therefore, the tentatively identified transformation products accounted for about 75% of the abated 2-ethynylbenzaldehyde



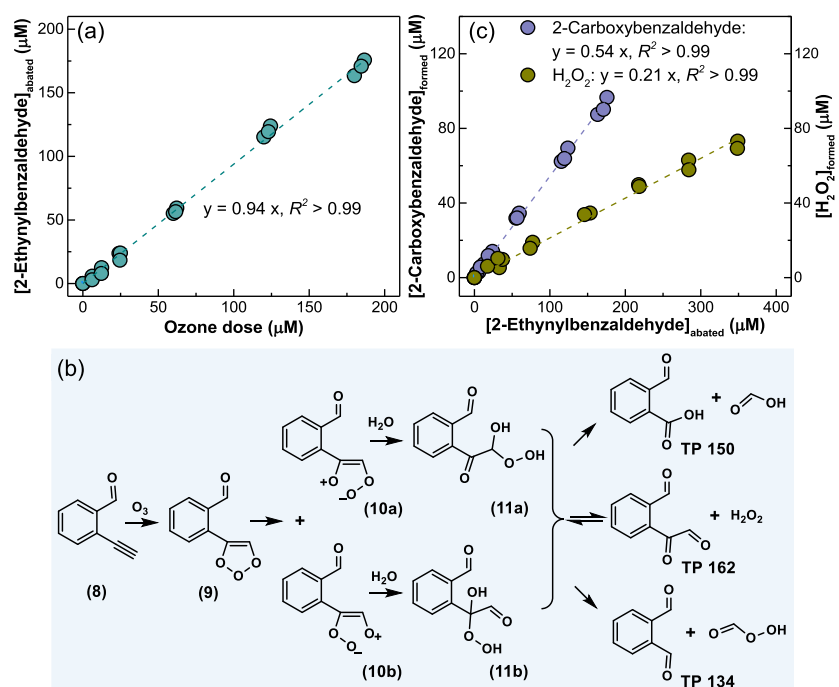


**Figure 4.** Reaction of ozone with 2-ethynylbenzaldehyde. (a) Stoichiometry of the reaction, (b) proposed transformation mechanism, and (c) 2-carboxybenzaldehyde (TP 150) and  $H_2O_2$  formation as functions of the abated 2-ethynylbenzaldehyde. Experimental conditions for stoichiometry and 2-carboxybenzaldehyde yield:  $[2\text{-ethynylbenzaldehyde}]_0 = 200 \mu\text{M}$ ,  $[O_3]_0 = 0\text{--}186 \mu\text{M}$ ,  $[t\text{-BuOH}]_0 = 20 \text{ mM}$ , pH 2.3, 10 mM phosphate buffer. Experimental conditions for  $H_2O_2$  yield:  $[2\text{-ethynylbenzaldehyde}]_0 = 500 \mu\text{M}$ ,  $[O_3]_0 = 0\text{--}640 \mu\text{M}$ ,  $[DMSO]_0 = 10 \text{ mM}$ , pH 2.3, 10 mM phosphate buffer.

(54% 2-carboxybenzaldehyde and 21% dicarbonyl compound TP 162).

**3.4.3. Reactivities of Representative Transformation Products with Ozone.** As shown in Figure S14,  $k_{O_3}$  for 2-carboxybenzaldehyde and phthalaldehyde at pH 2.3 were determined to be 0.16 and  $1.15 \text{ M}^{-1} \text{ s}^{-1}$ , respectively. Considering a  $pK_a$  of 4.57 for 2-carboxybenzaldehyde,<sup>73</sup> the measured second-order rate constant represents the species-specific second-order rate constant for the neutral form. Both transformation products are significantly less reactive than the parent compound, and therefore, they do not interfere with determination of the second-order rate constant for the ethynyl moiety in the parent compound and are also not significantly further degraded via ozone reactions. Nevertheless, further products can be formed due to  $\bullet\text{OH}$  reactions during ozonation of real waters.<sup>20,74</sup>

## 4. PRACTICAL IMPLICATIONS

The measured  $k_{O_3}$  values for olefins generally aligned with the reported data and followed the expected substituent effects. Water temperature is often unreported in the literature, allowing only rough comparisons between the measured and reported  $k_{O_3}$ . While olefins are electron-rich and typically susceptible to ozone attack, the presence of carbonyl, carboxyl, and alcohol groups significantly reduced their reactivities with ozone. Nevertheless, the measured  $k_{O_3}$  for such olefins are generally higher than those of extensively studied chlorinated olefins due to a stronger electron-withdrawing effect of chlorine.  $k_{O_3}$  for alkynes were determined to be approximately  $10^2 \text{ M}^{-1} \text{ s}^{-1}$ .

Seasonal changes in the water temperature can affect the efficiency of ozonation processes significantly. For olefins with

high  $k_{O_3}$  and low activation energies, changes in water temperature and hence ozone exposures have a limited effect on their abatement efficiency. In contrast, for alkynes with low  $k_{O_3}$  and high activation energies, a lower water temperature likely enhances their abatement if the residence times allow full ozone depletion. For the inactivation of *B. subtilis* spores at lower water temperature, the increased lag phase and reduced inactivation rate constant both lead to lower inactivation efficiency at the early stage of ozonation, while higher ozone exposure enhances inactivation at a later stage.

To achieve a 2-log inactivation of *B. subtilis* spores, ozone exposures of  $4.1 \times 10^{-3} \text{ Ms}$  at  $25^\circ\text{C}$  and  $1.8 \times 10^{-2} \text{ Ms}$  at  $5^\circ\text{C}$  are required, equivalent to ozone doses of about 0.91 and 0.75  $\text{mg L}^{-1}$  in Lake Zurich water (dissolved organic carbon concentration:  $1.3 \text{ mg L}^{-1}$ ),<sup>21</sup> respectively. Under these conditions, highly reactive compounds (e.g., olefins with  $k_{O_3} \geq 2 \times 10^3 \text{ M}^{-1} \text{ s}^{-1}$ ) can be completely abated (>99.9%) by ozone at both temperatures, while alkynes with  $k_{O_3} \approx 10^2 \text{ M}^{-1} \text{ s}^{-1}$  are only partially abated. For instance, 2-ethynylbenzaldehyde was calculated to be abated by 59% and 64% at 25 and  $5^\circ\text{C}$ , respectively. Compounds with low ozone reactivities (i.e.,  $k_{O_3} \leq 1 \text{ M}^{-1} \text{ s}^{-1}$ ) are barely affected (<2% abatement). Even though  $\bullet\text{OH}$  have limited impact on inactivation of *B. subtilis* spores, they could enhance the abatement of compounds with moderate and low ozone reactivities. This can be exemplified by increases in relative abatements of 59% to 68% for 2-ethynylbenzaldehyde and of 0.4% to 22% for a compound with  $k_{O_3} = 1 \text{ M}^{-1} \text{ s}^{-1}$  if  $\bullet\text{OH}$  reactions are also included, assuming a  $\bullet\text{OH}$ :ozone exposure ratio ( $R_{ct}$ ) of  $10^{-8}$  and  $k_{\bullet\text{OH}}$  of  $6 \times 10^9 \text{ M}^{-1} \text{ s}^{-1}$  at  $25^\circ\text{C}$ .

Various oxidative treatments of phenols lead to the formation of BDA. Despite the relatively high reactivity of the BDA isomers

with ozone ( $k_{\text{O}_3} > 10^3 \text{ M}^{-1} \text{ s}^{-1}$ ), this compound was still detected in a previous study during ozonation of wastewater for a relatively high specific ozone dose ( $\leq 3 \text{ mgO}_3/\text{mgC}$ ).<sup>31</sup> This suggests that the BDA formation is not completed at this point. The analysis of oxidation products reveals that the ozone reactions with olefins and alkynes primarily follow a Criegee-type mechanism, with minor alternative pathways reported in few cases.<sup>46</sup> The carbonyl product, glyoxal, formed from BDA ozonation, was observed to be effectively removed by biological post-treatment processes,<sup>75</sup> as was BDA,<sup>31</sup> and therefore, biological barriers as implemented after ozonation allow mitigation of these undesired compounds. For alkynes, carbonyl and carboxyl moieties are also formed on the core structure of the ethynyl group, and it is expected that these compounds are at least partially biodegradable.<sup>20</sup>

## ■ ASSOCIATED CONTENT

### SI Supporting Information

The Supporting Information is available free of charge at <https://pubs.acs.org/doi/10.1021/acs.est.4c07119>.

Reagents and solutions, details on reaction kinetics and analytical methods, measurement methods for target compounds and transformation products, synthesis and NMR analysis of BDA, and summary of second-order rate constants (PDF)

## ■ AUTHOR INFORMATION

### Corresponding Author

**Urs von Gunten** – School of Architecture, Civil and Environmental Engineering (ENAC), École Polytechnique Fédérale de Lausanne (EPFL), Lausanne 1015, Switzerland; Swiss Federal Institute of Aquatic Science and Technology, Eawag, Duebendorf 8600, Switzerland; Phone: +41-58-765-5270; Email: [urs.vongunten@eawag.ch](mailto:urs.vongunten@eawag.ch)

### Authors

**Yan Wang** – School of Architecture, Civil and Environmental Engineering (ENAC), École Polytechnique Fédérale de Lausanne (EPFL), Lausanne 1015, Switzerland; Key Laboratory of Drinking Water Science and Technology, Research Center for Eco-Environmental Sciences, Chinese Academy of Sciences, Beijing 100085, China; University of Chinese Academy of Sciences, Beijing 100049, China; [orcid.org/0009-0004-6550-8187](https://orcid.org/0009-0004-6550-8187)

**Eva M. Rodríguez** – School of Architecture, Civil and Environmental Engineering (ENAC), École Polytechnique Fédérale de Lausanne (EPFL), Lausanne 1015, Switzerland; Departamento de Ingeniería Química y Química Física, Universidad de Extremadura, Badajoz 06007, Spain

**Daniel Rentsch** – Swiss Federal Laboratories for Materials Testing and Research (EMPA), Duebendorf 8600, Switzerland; [orcid.org/0000-0002-9335-9527](https://orcid.org/0000-0002-9335-9527)

**Zhimin Qiang** – School of Environmental Science & Engineering, Shanghai Jiao Tong University, Shanghai 200240, China; [orcid.org/0000-0002-6555-3381](https://orcid.org/0000-0002-6555-3381)

Complete contact information is available at: <https://pubs.acs.org/doi/10.1021/acs.est.4c07119>

### Notes

The authors declare no competing financial interest.

## ■ ACKNOWLEDGMENTS

This study was financially supported by Chinese Scholarship Council (CSC), EPFL, Postdoctoral Fellowship Program of CPSF (GZC20232887), and China Postdoctoral Science Foundation (2024M753422). Y.W. gratefully thanks Caroline Gachet Aquillon, Tianqi Zhang, and Florian Breider for their help in analytical instrumentation and Joanna Houska and Minju Lee for discussion on ozone chemistry.

## ■ REFERENCES

- (1) Lim, S.; Shi, J. L.; von Gunten, U.; McCurry, D. L. Ozonation of organic compounds in water and wastewater: A critical review. *Water Res.* **2022**, *213*, 118053.
- (2) Huber, M. M.; Gobel, A.; Joss, A.; Hermann, N.; Löffler, D.; McArdell, C. S.; Ried, A.; Siegrist, H.; Ternes, T. A.; von Gunten, U. Oxidation of pharmaceuticals during ozonation of municipal wastewater effluents: a pilot study. *Environ. Sci. Technol.* **2005**, *39* (11), 4290–4299.
- (3) von Gunten, U. Oxidation processes and me. *Water Res.* **2024**, *253*, 121148.
- (4) von Sonntag, C.; von Gunten, U. *Chemistry of Ozone in Water and Wastewater Treatment. From Basic Principles to Applications*; IWA: London, 2012.
- (5) von Gunten, U. Ozonation of drinking water: part I. Oxidation kinetics and product formation. *Water Res.* **2003**, *37* (7), 1443–1467.
- (6) von Gunten, U. Oxidation processes in water treatment: Are we on track? *Environ. Sci. Technol.* **2018**, *52* (9), 5062–5075.
- (7) Houska, J.; Stocco, L.; Hofstetter, T. B.; von Gunten, U. Hydrogen peroxide formation during ozonation of olefins and phenol: Mechanistic insights from oxygen isotope signatures. *Environ. Sci. Technol.* **2023**, *57* (47), 18950–18959.
- (8) Kim, M. S.; Lee, C. Ozonation of microcystins: Kinetics and toxicity decrease. *Environ. Sci. Technol.* **2019**, *53* (11), 6427–6435.
- (9) Peter, A.; von Gunten, U. Oxidation kinetics of selected taste and odor compounds during ozonation of drinking water. *Environ. Sci. Technol.* **2007**, *41* (2), 626–631.
- (10) Genena, A. K.; Luiz, D. B.; Gebhardt, W.; Moreira, R. F. P. M.; José, H. J.; Schröder, H. F. Imazalil degradation upon applying ozone-transformation products, kinetics, and toxicity of treated aqueous solutions. *Ozone: Sci. Eng.* **2011**, *33* (4), 308–328.
- (11) Cruz-Alcalde, A.; Sans, C.; Esplugas, S. Priority pesticide dichlorvos removal from water by ozonation process: Reactivity, transformation products and associated toxicity. *Sep. Purif. Technol.* **2018**, *192*, 123–129.
- (12) Nikolaou, A. D.; Golinopoulos, S. K.; Kostopoulou, M. N.; Kolokythas, G. A.; Lekkas, T. D. Determination of volatile organic compounds in surface waters and treated wastewater in Greece. *Water Res.* **2002**, *36* (11), 2883–2890.
- (13) Burkhard, L. P.; Sheedy, B. R.; McCauley, D. J.; DeGraeve, G. M. Bioaccumulation factors for chlorinated benzenes, chlorinated butadienes and hexachloroethane. *Environ. Toxicol. Chem.* **1997**, *16* (8), 1677–1686.
- (14) LoPachin, R. M.; Gavin, T. Molecular mechanisms of aldehyde toxicity: A chemical perspective. *Chem. Res. Toxicol.* **2014**, *27* (7), 1081–1091.
- (15) Eder, E.; Hoffman, C.; Bastian, H.; Deininger, C.; Scheckenbach, S. Molecular mechanisms of DNA damage initiated by alpha, beta-unsaturated carbonyl compounds as criteria for genotoxicity and mutagenicity. *Environ. Health Perspect.* **1990**, *88*, 99–106.
- (16) Huber, M. M.; Ternes, T. A.; von Gunten, U. Removal of estrogenic activity and formation of oxidation products during ozonation of 17 $\alpha$ -ethynylestradiol. *Environ. Sci. Technol.* **2004**, *38* (19), 5177–5186.
- (17) Miller, D. J.; Nemo, T. E.; Hull, L. A. Rate study on the ozonolysis of acetylenes. *J. Org. Chem.* **1975**, *40* (18), 2675–2678.
- (18) Atkinson, R.; Carter, W. P. L. Kinetics and mechanisms of the gas-phase reactions of ozone with organic compounds under atmospheric conditions. *Chem. Rev.* **1984**, *84* (5), 437–470.

- (19) Demore, W. B. Rates and mechanism of alkyne ozonation. *Int. J. Chem. Kinet.* **1971**, *3* (2), 161–173.
- (20) Gulde, R.; Clerc, B.; Rutsch, M.; Helbing, J.; Salhi, E.; McArdell, C. S.; von Gunten, U. Oxidation of 51 micropollutants during drinking water ozonation: Formation of transformation products and their fate during biological post-filtration. *Water Res.* **2021**, *207*, 117812.
- (21) Elovitz, M. S.; von Gunten, U.; Kaiser, H. P. Hydroxyl radical/ozone ratios during ozonation processes. II. The effect of temperature, pH, alkalinity, and DOM properties. *Ozone: Sci. Eng.* **2000**, *22* (2), 123–150.
- (22) Hunt, N. K.; Mariñas, B. J. Kinetics of *Escherichia coli* inactivation with ozone. *Water Res.* **1997**, *31* (6), 1355–1362.
- (23) Driedger, A.; Staub, E.; Pinkernell, U.; Marinas, B.; Koster, W.; von Gunten, U. Inactivation of *Bacillus subtilis* spores and formation of bromate during ozonation. *Water Res.* **2001**, *35* (12), 2950–2960.
- (24) Wolf, C.; von Gunten, U.; Kohn, T. Kinetics of inactivation of waterborne enteric viruses by ozone. *Environ. Sci. Technol.* **2018**, *52* (4), 2170–2177.
- (25) Hoigné, J.; Bader, H. Rate constants of reactions of ozone with organic and inorganic compounds in water-I: non-dissociating organic compounds. *Water Res.* **1983**, *17* (2), 173–183.
- (26) Huber, M. M.; Canonica, S.; Park, G. Y.; von Gunten, U. Oxidation of pharmaceuticals during ozonation and advanced oxidation processes. *Environ. Sci. Technol.* **2003**, *37* (5), 1016–1024.
- (27) Dowd, P.; von Sonntag, C. Reaction of ozone with ethene and its methyl- and chlorine-substituted derivatives in aqueous solution. *Environ. Sci. Technol.* **1998**, *32* (8), 1112–1119.
- (28) Atkins, P.; de Paula, J.; Keeler, J. *Atkins' Physical Chemistry*, 11th ed.; Oxford University Press: Oxford, United Kingdom, 2018.
- (29) Hansen, E. W.; Holm, K. H.; Jahr, D. M.; Olafsen, K.; Stori, A. Reaction of poly(vinyl alcohol) and dialdehydes during gel formation probed by  $^1\text{H}$  n.m.r.-a kinetic study. *Polymer* **1997**, *38* (19), 4863–4871.
- (30) Hensley, J. C.; Birdsall, A. W.; Valtierra, G.; Cox, J. L.; Keutsch, F. N. Revisiting the reaction of dicarbonyls in aerosol proxy solutions containing ammonia: The case of butenedial. *Atmos. Chem. Phys.* **2021**, *21* (11), 8809–8821.
- (31) Houska, J.; Manasfi, T.; Gebhardt, I.; von Gunten, U. Ozonation of lake water and wastewater: Identification of carbonous and nitrogenous carbonyl-containing oxidation byproducts by non-target screening. *Water Res.* **2023**, *232*, 119484.
- (32) Marron, E. L.; Prasse, C.; Buren, J. V.; Sedlak, D. L. Formation and fate of carbonyls in potable water reuse systems. *Environ. Sci. Technol.* **2020**, *54* (17), 10895–10903.
- (33) Acero, J. L.; von Gunten, U. Influence of carbonate on the ozone/hydrogen peroxide based advanced oxidation process for drinking water treatment. *Ozone: Sci. Eng.* **2000**, *22* (3), 305–328.
- (34) Yurkova, I. L.; Schuchmann, H.-P.; von Sonntag, C. Production of OH radicals in the autoxidation of the Fe(II)–EDTA system. *J. Chem. Soc., Perkin Trans. 2* **1999**, No. 10, 2049–2052.
- (35) Stocco, L. Quantification of ozone-reactive precursors in dissolved organic matter: Formation of  $\text{H}_2\text{O}_2$  and its transformation to  $\text{O}_2$  for isotope ratio analysis, Master's Thesis EPFL, 2021. <https://infoscience.epfl.ch/record/295199>.
- (36) Bader, H.; Hoigné, J. Determination of ozone in water by the indigo method. *Water Res.* **1981**, *15* (4), 449–456.
- (37) Yao, C. C. D.; Haag, W. R. Rate constants for direct reactions of ozone with several drinking-water contaminants. *Water Res.* **1991**, *25* (7), 761–773.
- (38) *Handbook of Chemistry and Physics*, 71st. ed.; Lide, D. K., Ed.; CRC Press: Boca Raton, FL, 1991; pp: 8–35.
- (39) Leitzke, A.; Reisz, E.; Flyunt, R.; von Sonntag, C. The reactions of ozone with cinnamic acids: formation and decay of 2-hydroperoxy-2-hydroxyacetic acid. *J. Chem. Soc., Perkin Trans. 2* **2001**, No. 5, 793–797.
- (40) Jans, U. Radikalbildung aus Ozon in atmosphärischen Wassern—Einfluss von Licht, gelösten Stoffen und Russpartikeln, Doctoral Thesis ETHZ 11814, 1996.
- (41) Witkowski, B.; Al-Sharafi, M.; Gierczak, T. Kinetics of limonene secondary organic aerosol oxidation in the aqueous phase. *Environ. Sci. Technol.* **2018**, *52* (20), 11583–11590.
- (42) Taft, R. W. Separation of polar, steric and resonance effects in reactivity. In *Steric Effects in Organic Chemistry*; Newman, M. S., Ed.; John Wiley & Sons: New York, 1956.
- (43) Hoigné, J.; Bader, H. Rate constants of reactions of ozone with organic and inorganic compounds in water-II: dissociating organic compounds. *Water Res.* **1983**, *17* (2), 185–194.
- (44) Benbelkacem, H.; Cano, H.; Mathe, S.; Debellefontaine, H. Maleic acid ozonation: Reactor modeling and rate constants determination. *Ozone: Sci. Eng.* **2003**, *25* (1), 13–24.
- (45) Pryor, W. A.; Giamalva, D. H.; Church, D. F. Kinetics of ozonation. 2. Amino acids and model compounds in water and comparisons to rates in nonpolar solvents. *J. Am. Chem. Soc.* **1984**, *106* (23), 7094–7100.
- (46) Leitzke, A.; von Sonntag, C. Ozonolysis of unsaturated acids in aqueous solution: Acrylic, methacrylic, maleic, fumaric and muconic acids. *Ozone: Sci. Eng.* **2009**, *31* (4), 301–308.
- (47) Benbelkacem, H.; Mathé, S.; Benbelkacem, H. Taking mass transfer limitation into account during ozonation of pollutants reacting fairly quickly. *Water Sci. Technol.* **2004**, *49* (4), 25–30.
- (48) Navon, N.; Masarwa, A.; Cohen, H.; Meyerstein, D. pH dependence of the stability constants of copper(I) complexes with fumaric and maleic acids in aqueous solutions. *Inorg. Chim. Acta* **1997**, *261* (1), 29–35.
- (49) Batchelor, J. G.; Feeney, J.; Roberts, G. C. K. Carbon-13 NMR protonation shifts of amines, carboxylic acids and amino acids. *J. Magn. Reson.* **1975**, *20* (1), 19–38.
- (50) Lee, M.; Merle, T.; Rentsch, D.; Canonica, S.; von Gunten, U. Abatement of polychloro-1,3-butadienes in aqueous solution by ozone, UV photolysis, and advanced oxidation processes ( $\text{O}_3/\text{H}_2\text{O}_2$  and  $\text{UV}/\text{H}_2\text{O}_2$ ). *Environ. Sci. Technol.* **2017**, *51* (1), 497–505.
- (51) Pitzer, K. S.; Hollenberg, J. L. *cis*- and *trans*-Dichloroethylenes. The infrared spectra from 130–400  $\text{cm}^{-1}$  and the thermodynamic properties<sup>1</sup>. *J. Am. Chem. Soc.* **1954**, *76* (6), 1493–1496.
- (52) Chaudhuri, R. K.; Hammond, J. R.; Freed, K. F.; Chattopadhyay, S.; Mahapatra, U. S. Reappraisal of *cis* effect in 1,2-dihaloethenes: An improved virtual orbital multireference approach. *J. Chem. Phys.* **2008**, *129* (6), 064101.
- (53) Silver, B. L.; Luz, Z.; Peller, S.; Reuben, J. Intramolecular hydrogen bonding in the hydrogen anions of some carboxylic acids in water and water-methanol mixtures. Evidence from proton magnetic resonance. *J. Phys. Chem.* **1966**, *70* (5), 1434–1440.
- (54) Pedersen, T.; Sehested, K. Rate constants and activation energies for ozonolysis of isoprene methacrolein and methyl-vinyl-ketone in aqueous solution: Significance to the in-cloud ozonation of isoprene. *Int. J. Chem. Kinet.* **2001**, *33* (3), 182–190.
- (55) Theruvathu, J. A.; Flyunt, R.; Aravindakumar, C. T.; von Sonntag, C. Rate constants of ozone reactions with DNA, its constituents and related compounds. *J. Chem. Soc., Perkin Trans. 2* **2001**, No. 3, 269–274.
- (56) Onstad, G. D.; Strauch, S.; Meriluoto, J.; Codd, G. A.; von Gunten, U. Selective oxidation of key functional groups in cyanotoxins during drinking water ozonation. *Environ. Sci. Technol.* **2007**, *41* (12), 4397–4404.
- (57) Keady, H. D.; Kuo, C. H. A data acquisition system for rapid kinetic experiments. *Chem. Eng. Commun.* **1983**, *23* (4–6), 291–304.
- (58) Levis, D. H.; Van Ry, D. A.; Hinrichs, R. Z. Multiphase ozonolysis of aqueous  $\alpha$ -terpineol. *Environ. Sci. Technol.* **2016**, *50* (21), 11698–11705.
- (59) Tekle-Röttering, A.; Lim, S.; Reisz, E.; Lutze, H. V.; Abdighahroudi, M. S.; Willach, S.; Schmidt, W.; Tentscher, P. R.; Rentsch, D.; McArdell, C. S.; Schmidt, T. C.; von Gunten, U. Reactions of pyrrole, imidazole, and pyrazole with ozone: kinetics and mechanisms. *Environ. Sci. Water Res. Technol.* **2020**, *6* (4), 976–992.
- (60) Arena, G.; Cali, R.; Maccarone, E.; Passerini, A. Thermodynamics of protonation of some five-membered heteroaryl-carboxylates,



-alkanoates and -*trans*-propenoates. *J. Chem. Soc., Perkin Trans. 2* **1993**, No. 10, 1941.

(61) Chemical book. CAS database list for CAS No. 3238–40–2, furan-2,5-dicarboxylic acid, 2023. <https://www.chemicalbook.com/ProductChemicalPropertiesCB6264091.htm> (accessed Nov 10, 2023).

(62) Zoumpoulis, G. A.; Zhang, Z. Y.; Wenk, J.; Prasse, C. Aqueous ozonation of furans: Kinetics and transformation mechanisms leading to the formation of  $\alpha,\beta$ -unsaturated dicarbonyl compounds. *Water Res.* **2021**, *203*, 117487.

(63) Lee, Y.; von Gunten, U. Quantitative structure–activity relationships (QSARs) for the transformation of organic micro-pollutants during oxidative water treatment. *Water Res.* **2012**, *46*, 6177–6195.

(64) Morsch, L.; Farmer, S.; Cunningham, K.; Sharrett, Z. Organic chemistry. The open education resource (OER) libretexts project, 2024. [https://chem.libretexts.org/Bookshelves/Organic\\_Chemistry/Organic\\_Chemistry\\_\(Morsch\\_et\\_al.\)/01:\\_Structure\\_and\\_Bonding/1.09:\\_sp\\_Hybrid\\_Orbitals\\_and\\_the\\_Structure\\_of\\_Acetylene](https://chem.libretexts.org/Bookshelves/Organic_Chemistry/Organic_Chemistry_(Morsch_et_al.)/01:_Structure_and_Bonding/1.09:_sp_Hybrid_Orbitals_and_the_Structure_of_Acetylene) (accessed April 22, 2024).

(65) Nicolaides, A.; Borden, W. T. Ab initio calculations of the relative strengths of the  $\pi$  bonds in acetylene and ethylene and of their effect on the relative energies of  $\pi$ -bond addition reactions. *J. Am. Chem. Soc.* **1991**, *113* (18), 6750–6755.

(66) Chemical book. CAS database list for CAS No. 2345–51–9, 3-butynoic acid, 2023. [https://www.chemicalbook.com/ChemicalProductProperty\\_EN\\_CB4500119.htm](https://www.chemicalbook.com/ChemicalProductProperty_EN_CB4500119.htm) (accessed Nov 10, 2023).

(67) Crawford, M. Chem. 321: Physical chemistry. The open education resource (OER) libretexts project, 2023. [https://chem.libretexts.org/Courses/Knox\\_College/Chem\\_321:\\_Physical\\_Chemistry\\_I/12:\\_Chemical\\_Equilibrium/12.05:\\_The\\_Van't\\_Hoff\\_Equation](https://chem.libretexts.org/Courses/Knox_College/Chem_321:_Physical_Chemistry_I/12:_Chemical_Equilibrium/12.05:_The_Van't_Hoff_Equation) (accessed Dec 15, 2023).

(68) Das, R. C.; Dash, U. N.; Panda, K. N. Thermodynamics of the dissociation of *trans*-cinnamic acid. *Can. J. Chem.* **1976**, *54* (12), 1916–1917.

(69) Prasse, C.; Ford, B.; Nomura, D. K.; Sedlak, D. L. Unexpected transformation of dissolved phenols to toxic dicarbonyls by hydroxyl radicals and UV light. *Proc. Natl. Acad. Sci. U.S.A.* **2018**, *115* (10), 2311–2316.

(70) Prasse, C.; von Gunten, U.; Sedlak, D. L. Chlorination of phenols revisited: Unexpected formation of  $\alpha,\beta$ -unsaturated  $C_4$ -dicarbonyl ring cleavage products. *Environ. Sci. Technol.* **2020**, *54* (2), 826–834.

(71) Bothe, E.; Schultefrohlinde, D. Reaction of dihydroxymethyl radical with molecular-oxygen in aqueous-solution. *Z. Naturforsch. B* **1980**, *35* (8), 1035–1039.

(72) Rath, S. A.; von Gunten, U. Achieving realistic ozonation conditions with synthetic water matrices comprising low-molecular-weight scavenger compounds. *Water Res.* **2024**, *261*, 121917.

(73) Chemical book. CAS database list for CAS No. 119–67–5, 2-carboxybenzaldehyde, 2023. [https://www.chemicalbook.com/ChemicalProductProperty\\_EN\\_CB7146219.htm](https://www.chemicalbook.com/ChemicalProductProperty_EN_CB7146219.htm) (accessed Nov 10, 2023).

(74) Gulde, R.; Rutsch, M.; Clerc, B.; Schollée, J. E.; von Gunten, U.; McArde, C. S. Formation of transformation products during ozonation of secondary wastewater effluent and their fate in post-treatment: From laboratory- to full-scale. *Water Res.* **2021**, *200*, 117200.

(75) Manasfi, T.; Houska, J.; Gebhardt, I.; von Gunten, U. Formation of carbonyl compounds during ozonation of lake water and wastewater: Development of a non-target screening method and quantification of target compounds. *Water Res.* **2023**, *237*, 119751.